Energetic decomposition of modes in resistive plasmas

J. Puchmayr[1], M. Dunne[1], E. Strumberger[1]

[1] *Max Planck Institute for Plasma Physics, Boltzmannstr. 2, 85748 Garching, Germany*

Magnetohydrodynamic (MHD) instabilities can significantly decrease energy and particle confinement of fusion plasmas. Consequently, the understanding of MHD stability is crucial for the design and operation of future fusion devices. While there are analytical descriptions of MHD stability for simple plasma configurations or in certain limits, the MHD stability analysis of realistic, more complex plasma configurations requires numerical solutions of the MHD equations. The numerical solution for a single plasma configuration yields the growth rate and structure of instabilities. Studying MHD stability of multiple plasmas grants information on trends with different plasma parameters (e.g. plasma current). For ideal modes, additional information on the physics driving these instabilities can be obtained using the energy functional as derived by Greene and Johnson [1], which separates the energetic contributions into pressure drive, current drive and stabilizing terms. However, for some plasmas and types of instability finite resistivity must be taken into account. In order to analyze the energetic composition of modes in resistive plasmas, we extend the energy functional by Greene and Johnson to the regime of finite resistivity. The resulting resistive energy functional grants additional insight for numerical solutions but is not in the form of a solvable eigenvalue problem. We have implemented the resistive energy functional in the linear stability code CASTOR3D and validated it for a simple test case using three different coordinate systems.

Starting from the set of linearized MHD equations as implemented in the CASTOR3D code [2, 3], the plasma energy is obtained by multiplication of the linearized momentum equation with $\frac{1}{2}\vec{\xi}^*$ and integration over the plasma volume, where we introduce the plasma displacement $\vec{\xi}$ by $\partial_t\vec{\xi} = \vec{v}_1$ and the perturbed velocity $\vec{v}_1$. Integrating by parts, applying vector algebra and using the linearized resistive MHD equations analogously to Bernstein et al. and Greene and Johnson [1, 4], the energy functional for resistive plasma perturbations reads (see [5]):

$$2\delta W = 2\delta W_V + 2\delta W_S + 2\delta W_{\hat{V}} = -\int \rho_0 \lambda^2 |\vec{\xi}|^2 \mathrm{dV} \tag{1}$$

where we separate surface δW_S, vacuum $\delta W_{\hat{V}}$ and plasma volume δW_V contributions

$$2\delta W_S = \oint |\vec{n}\cdot\vec{\xi}|^2\, \vec{n}\cdot\left[\!\left[\vec{\nabla}(p_0 + \frac{\vec{B}_0^2}{2\mu_0})\right]\!\right] \mathrm{dS}\,, \quad 2\delta W_{\hat{V}} = \int \frac{|\hat{\vec{B}}_1|^2}{\mu_0}\mathrm{d\hat{V}} \tag{2}$$

and

$$
\begin{aligned}
2\delta W_V \;=\; & \underbrace{\int \frac{|\vec{B}_{1,\perp}|^2}{\mu_0}\mathrm{dV}}_{W_{\mathrm{SHA}}} + \underbrace{\int \frac{\vec{B}_0^2}{\mu_0}\left|\vec{\nabla}\cdot\vec{\xi}_\perp + 2(\vec{\xi}_\perp\cdot\vec{\kappa}) + \frac{1}{\vec{B}_0^2}\vec{B}_0\cdot\vec{B}_R\right|^2\mathrm{dV}}_{W_{\mathrm{CPA}}} \\
& \underbrace{+\Gamma\int p_0|\vec{\nabla}\cdot\vec{\xi}|^2\mathrm{dV}}_{W_{\mathrm{SND}}} \qquad \underbrace{+\frac{1}{\mu_0^2\lambda^*}\int \eta|\vec{\nabla}\times\vec{B}_1|^2\mathrm{dV}}_{W_{\mathrm{RCD}}} \\
& \underbrace{-\int \frac{j_{0,\parallel}}{|\vec{B}_0|}(\vec{\xi}_\perp^{\,*}\times\vec{B}_0)\cdot\vec{B}_{1,\perp}\mathrm{dV}}_{W_{\mathrm{CUR}}} \qquad \underbrace{-\int 2(\vec{\xi}_\perp\cdot\vec{\nabla}p_0)(\vec{\xi}_\perp^{\,*}\cdot\vec{\kappa})\mathrm{dV}}_{W_{\mathrm{DP0}}} \\
& \underbrace{-\int \frac{1}{\vec{B}_0^2}(\vec{\xi}_\parallel^{\,*}\times\vec{\nabla}p_0)\cdot(\vec{B}_0\times\vec{B}_R)\mathrm{dV}}_{W_{\mathrm{RD},\parallel}} \qquad \underbrace{-\int \frac{1}{\vec{B}_0^2}(\vec{\xi}_\perp\cdot\vec{\nabla}p_0)(\vec{B}_0\cdot\vec{B}_R^{\,*})\mathrm{dV}}_{W_{\mathrm{RD},\perp}}
\end{aligned}
\tag{3}
$$

with density ρ, pressure p, current density $\vec{j}$, magnetic field $\vec{B}$, resistivity η, adiabatic coefficient Γ, surface normal vector of the plasma volume $\vec{n}$, the linear growth rate or eigenvalue $\lambda \in \mathbb{C}$, field-line-curvature vector $\vec{\kappa} = (\vec{b}\cdot\vec{\nabla})\vec{b}$ with $\vec{b} = \vec{B}_0/|\vec{B}_0|$ and ohmic field $\vec{B}_R = \lambda^{-1}\vec{\nabla}\times(\eta\vec{j}_1)$. The parallel current density is given by $j_{0,\parallel} = (\vec{j}_0\cdot\vec{B}_0)/|\vec{B}_0|$. Equilibrium and perturbed quantities are distinguished by indices 0 and 1, respectively. Hats denote vacuum quantities, $\parallel$ and $\perp$ denote parallel and perpendicular components w.r.t. $\vec{B}_0$ and $[\![\ldots]\!]$ denotes the jump of the enclosed quantities across the plasma boundary.

The different forms of energy which determine the growth of a mode are related to perpendicular magnetic perturbations W_{SHA}, parallel magneto-compressional perturbations W_{CPA}, adiabatic plasma compression W_{SND}, resistive current diffusion W_{RCD}, parallel current-density drive W_{CUR}, field-line-curvature dependent pressure-gradient drive W_{DP0} and resistive corrections to the pressure gradient drive $W_{\mathrm{RD},\parallel}$ and $W_{\mathrm{RD},\perp}$. The first four terms (W_{SHA}, W_{CPA}, W_{SND}, W_{RCD}) as well as the vacuum contribution $\delta W_{\hat{V}}$ are always stabilizing. The resistive corrections $W_{\mathrm{RD},\parallel}$ and $W_{\mathrm{RD},\perp}$ account for the effect of resistive diffusion on the work done by the induced magnetic perturbation which is generated by parallel and perpendicular compression of the plasma, respectively. The surface contribution δW_S is zero if there are no equilibrium surface currents. In summary, three new resistive terms (W_{RCD}, $W_{\mathrm{RD},\parallel}$, $W_{\mathrm{RD},\perp}$) as well as a resistive correction to the energy of parallel magneto-compressional perturbations W_{CPA} must be considered for resistive plasma perturbations (highlighted terms in equation (Eq. 3)). The vacuum and surface contributions are not affected by finite values of resistivity.

We implemented the resistive energy functional in the CASTOR3D code in general 3D curvilinear coordinates. The energy functional is validated by comparison of potential and

kinetic energy of an $n = 8$ Edge Localized Mode in a simple low-β axisymmetric test equilibrium across three different coordinate systems: NEMEC coordinates (NEM), 2D straight field line coordinates (SFL) and Boozer coordinates (BZR). The pressure and safety factor profiles of the test equilibrium are shown in figure (Fig. 1a). The test resistivity profile $\eta(r) = \frac{\eta_b}{221} \cdot (1 + 10r + 10r^2 + 100r^8 + 100r^{10})$, shown in figure (Fig. 1b), is defined to be large at the plasma edge and small in the center, where r is the square-root of the normalized toroidal flux and η_b is the resistivity at the plasma boundary.

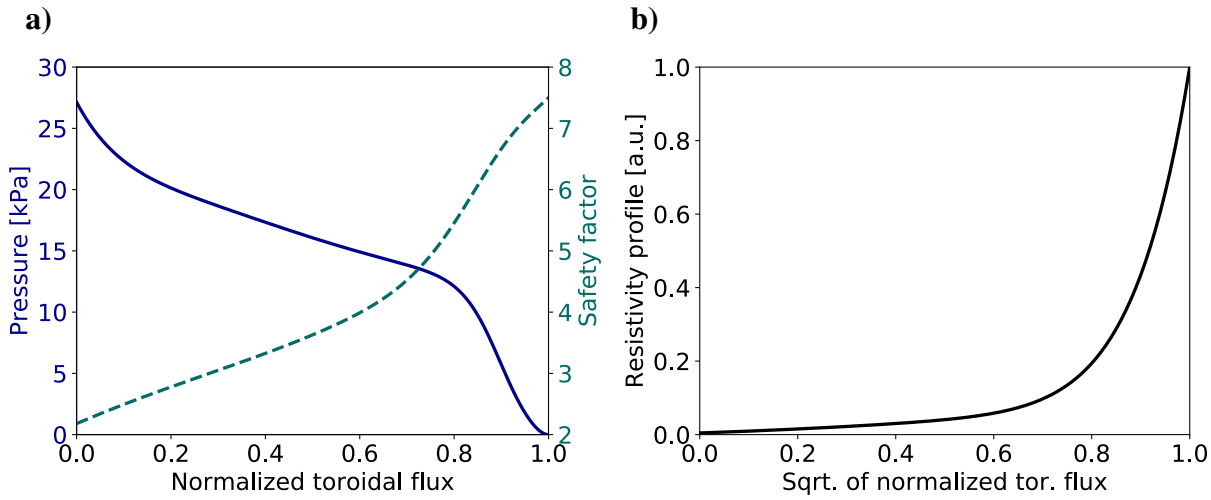

Figure 1: *a) Pressure (solid) and safety factor (dashed) profiles of the test equilibrium. b) Shape of the test resistivity profile.*

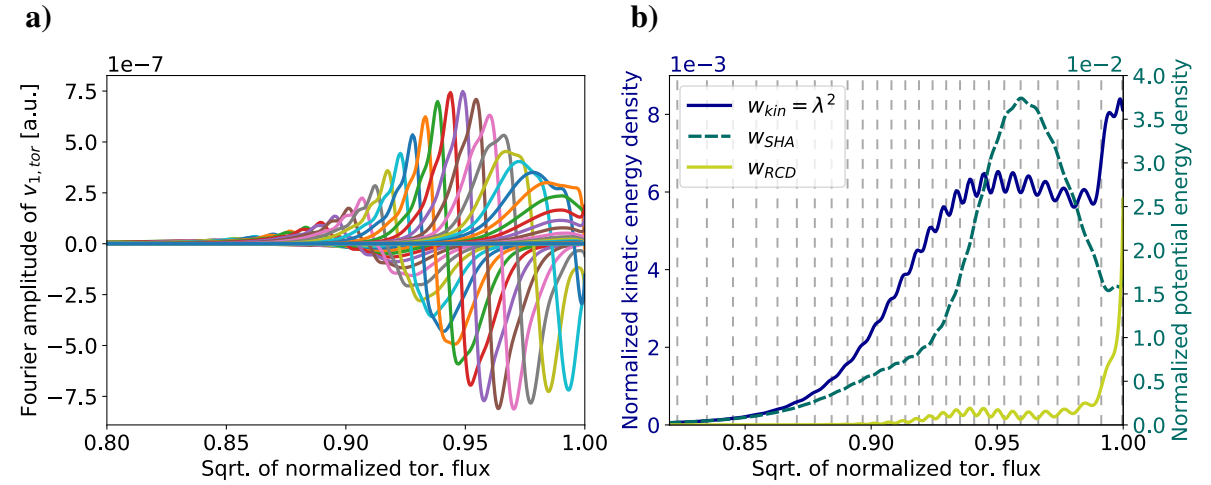

Figure 2: *a) Fourier spectrum (BZR) of the perturbed toroidal velocity. b) Normalized energy densities corresponding to* $W_{kin} = \int \rho_0 \lambda^2 |\vec{\xi}|^2 dV$, W_{SHA} *and* W_{RCD} *for the validation case (BZR).*

The Fourier spectrum of the toroidal velocity perturbation (BZR) is shown in figure (Fig. 2a) for the test mode. As a result of the validation (see [5]), the sum of the potential energy terms of the perturbation matches the kinetic energy within bounds of -0.06% (NEM), 0.91% (SFL) and 0.37% (BZR) for the test case with $\eta_b = 2.21 \cdot 10^6$ Ωm, validating that all potential energy

terms have been considered and the functional was implemented correctly in the general 3D formulation of CASTOR3D. The accurate calculation of the energy terms requires well-converged eigenfunctions and equilibria as well as a radial resolution which is sufficient to resolve the resonant flux surfaces, as can be seen in figure (Fig. 2b). A sufficiently large number of poloidal and toroidal mode numbers must be provided for the Fourier representation of the mode in order to ensure convergence of the eigenfunction. Well-converged equilibria correspond to small errors in the force balance and are necessary for validity of the linear equations.

In order to compare the energy compositions of different perturbations and to measure the impact of the resistive corrections, we define proportions of the potential energy terms:

$$\chi_{\mathrm{RCD}} = W_{\mathrm{RCD}}/(W_{\mathrm{RCD}} + W_{\mathrm{SHA}} + W_{\mathrm{CPA}} + W_{\mathrm{SND}}) \tag{4}$$

$$\chi_{\mathrm{RD}} = (W_{\mathrm{RD},\perp} + W_{\mathrm{RD},\parallel})/(W_{\mathrm{RD},\perp} + W_{\mathrm{RD},\parallel} + W_{\mathrm{DP0}}) \tag{5}$$

$$\chi_{\mathrm{DP/CUR}} = (W_{\mathrm{RD},\perp} + W_{\mathrm{RD},\parallel} + W_{\mathrm{DP0}})/(W_{\mathrm{RD},\perp} + W_{\mathrm{RD},\parallel} + W_{\mathrm{DP0}} + W_{\mathrm{CUR}}) \tag{6}$$

which are shown for the test perturbation over a range of resistivity values in figure (Fig. 3). One can see that resistive corrections are even important at realistic values of resistivity and for ideal instabilities, i.e. finite growth rate for $\eta \to 0$. For larger values of resistivity the test mode becomes more pressure gradient driven ($\chi_{\mathrm{DP/CUR}}$) and the energy absorbed by resistive current diffusion dominates the stabilizing contributions.

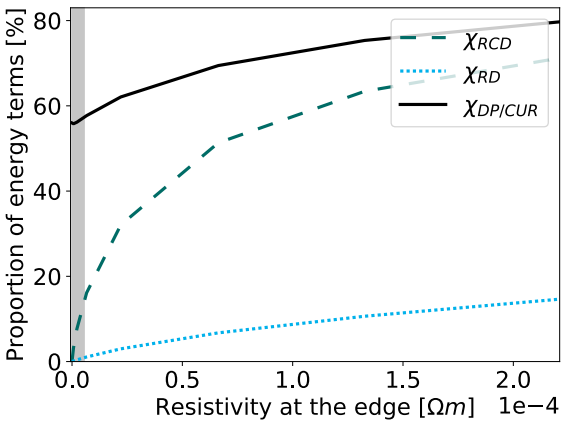

Figure 3: *Proportions of potential energy terms for the test mode over a range of resistivity values. Gray area: Realistic values of resistivity.*

In conclusion, we have extended the energy functional separating pressure drive, current-density drive and stabilizing terms to the regime of finite resistivity, implemented the resistive energy functional in the CASTOR3D code and validated it for a simple test case across three different coordinate systems. A method to evaluate the energy composition as well as a scan of the test case over a range of resistivity values was presented.

References

[1] J. M. Greene and J. L. Johnson, Plasma Physics **10**, 729 (1968)

[2] E. Strumberger and S. Günter, Nucl. Fusion **57**, 016032 (2017)

[3] E. Strumberger and S. Günter, Nucl. Fusion **59**, 106008 (2019)

[4] I. B. Bernstein, E. A. Frieman, M. D. Kruskal and R. M. Kulsrud, Proc. R. Soc. Lond. **244**, 17 (1958)

[5] J. Puchmayr, M. Dunne and E. Strumberger, *Submitted to* Journal of Plasma Physics